STUDY OF DEPTH PROFILE OF INDENTATION CRACKS IN SILICON NITRIDE

ERNEST GONDÁR[1]*, MIROSLAV ROŠKO[1], MILINA ZEMÁNKOVÁ[2]

[1] *Department of Materials and Technology, Faculty of Mechanical Engineering, Slovak University of Technology, Pionierska 15, 812 31 Bratislava, Slovak Republic*
[2] *Institute of Materials and Machine Mechanics, Slovak Academy of Sciences, Račianska 75, 831 02 Bratislava, Slovak Republic*

Received 28 May 2004, accepted 20 October 2004

The depth profile of indentation cracks has been determined by removing thin layers from the specimen by serial sectioning, as well as from observation of fracture areas after breaking of the specimens. A considerably defective deformed area has been identified under the indent, depth of which ranges from 120 to 140 μm. The shape of the deformed area is of angular, pyramid-like type. At the interface of the deformed and non-deformed area, minor cracks have been observed. The length of these minor cracks is much shorter when compared with the length of the major ones, however, they are more numerous. The volumes of the indents and the deformed areas have been compared for all of the indents. It follows from the calculations that the volume of the indent represents on average 8 % of the volume of deformed area.

K e y w o r d s: silicon nitride, deformation under indent, depth profile of cracks, serial sectioning, fracture area

1. Introduction

An important position of silicon nitride in the industry is given by its properties, especially by its hardness and wear resistance, room and high-temperature strength and by its resistance to corrosion and creep [1–3]. Its resistance to repeated thermal shocks often determines the possibility of high-temperature applications of Si_3N_4. In the Department of Materials and Technologies of the Faculty of Mechanical Engineering of the Slovak Technical University, a new testing method has been developed to test the resistance of silicon nitride to repeated thermal shocks [4, 5], using samples with cracks initiated by Vickers indentor. Along with this testing method, a computing model is being developed to simulate the temperatures and stresses developed in the specimen under the conditions of repeated thermal

*corresponding author, e-mail: ernest.gondar@stuba.sk

shocks. For the modelling purposes it is necessary to know the depth profile of the initiated cracks. The study of the indentation cracks in structural ceramics and also in silicon nitride has been the subject of many investigations during the last decades [6, 7]. Study of the depth profile in Si_3N_4 with Y_2O_3 and Al_2O_3 additives is the subject of this contribution.

2. Experiment

The specimens were prepared by cold pressing and then hot pressing in nitrogen (N_2) atmosphere. Sintering additives of silicon nitride were Al_2O_3 and Y_2O_3 with mass ratio [8]: 85.36 wt.% Si_3N_4 + 10.34 wt.% Y_2O_3 + 4.30 wt.% Al_2O_3. This mass ratio corresponds to 10 % YAG.

The hot pressing of the experimental material was performed on a laboratory hot press with a special construction of heating body [9].

The prepared specimens were of 2 mm thickness with 8 mm diameter. After metallographic preparation of the specimens, cracks were initiated into them using Vickers hardness tester HPO250 with following parameters: loading force $F = 294.3$ N, loading time $t = 15$ s and temperature $T = 20\,℃$.

The depth profiles of cracks under the indents were observed on 2 specimens, with 6 indents indented into each of them. Since two cracks were initiated at each indent, the total number of observed depth profiles was 24. The depth profile of the cracks is determined by serial sectioning (layer-by-layer removal) of the material, as well as from the observation of fracture areas. The number of ablated indents was 12, number of observed fracture areas was 10.

The ablation was performed on laboratory grinding discs using devices Pedemin-S and Dap-V. First, the specimens were ground for 2 minutes using a disc with granularity of 40 μm. Afterwards, discs with diamond pastes of granularity 10/7, 5/3 and 1/0 were used to polish the surface. Up to 30 ablations and measurements were made for each specimen.

The thickness of ablated layers was determined by measuring the diagonals of the indent (Fig. 1) using a formula:

$$H = \frac{\frac{L1 - L2}{2}}{\mathrm{tg}\,\frac{136^\circ}{2}}, \tag{1}$$

where $L1$ is length of the diagonal before ablating [μm], $L2$ is length of the diagonal after ablating [μm].

Since the measuring of diagonals of the indents was the only way to determine the depth of ablating, a complete removal of the indent would mean the loss of depth reference. To prevent this, new indents had been indented into the specimen before ablating the old ones. This way, we were always able to measure diagonals of the indents and thus we always had correct information on the depth of ablating.

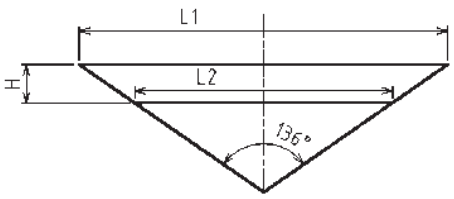

Fig. 1. Geometry of the indent.

3. Results and discussion

The stepwise change of measured areas is shown in Fig. 2 (sketch) and Fig. 3 (ceramographic sections). In these figures, step 0 represents the original state, before ablating. Step 1 represents a depth with indent still present and step 2 represents ablation in a depth close under the indent. In steps 1 and 2 it can be seen, that the inner ends of the cracks are not connected – they connect deeper under the surface, in step 3. This demonstrates the presence of a deformed area under the indent. It can be assumed, that in this area there was a higher compaction of the

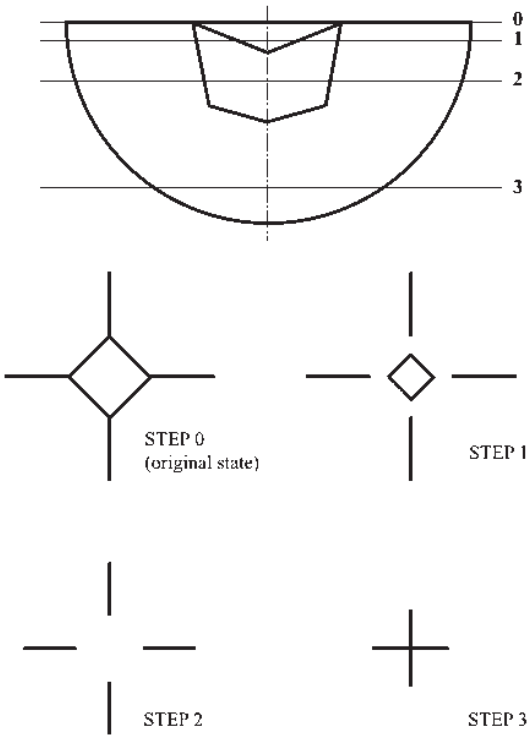

Fig. 2. The steps (0–3) of serial sectioning – sketch.

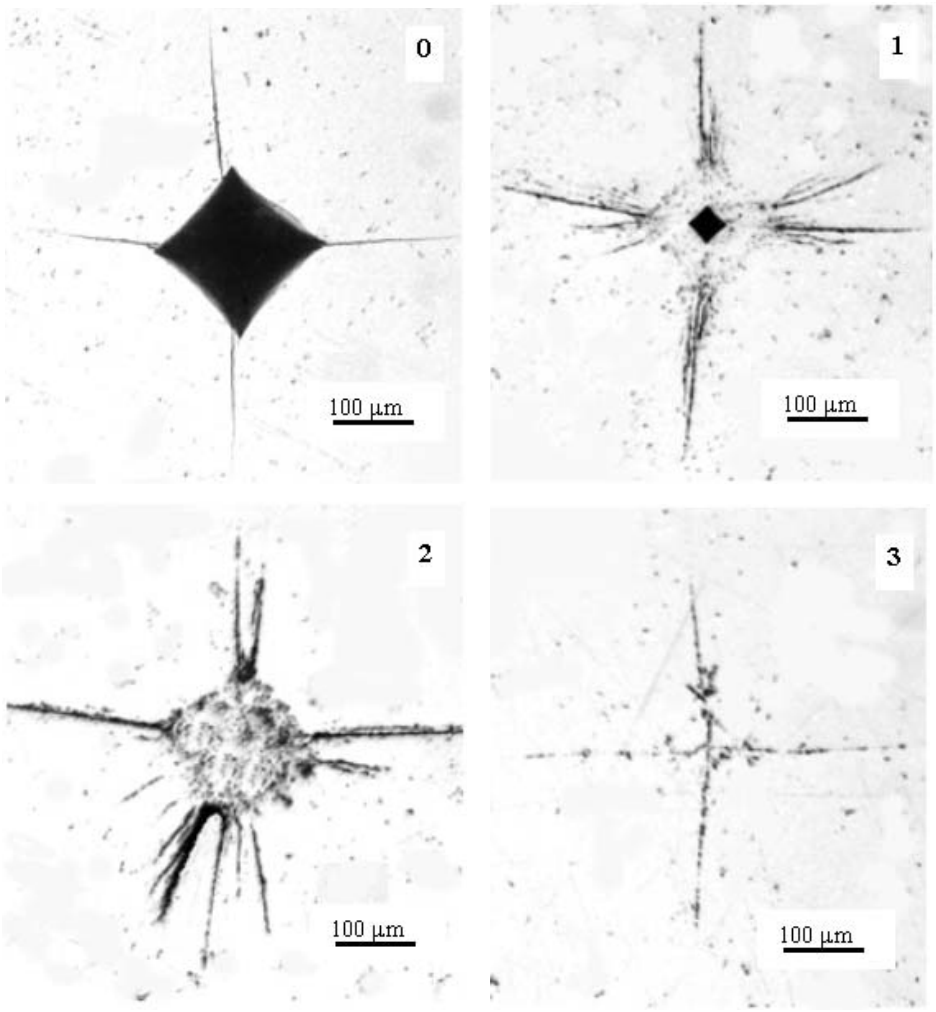

Fig. 3. The steps (0–3) of serial sectioning – ceramographic sections.

material and the crack progress has been stopped. In Fig. 3 (step 1) it can be seen, that the shape of the deformed area copies the shape of the indent. This angular shape remains also after removing the indent (step 2). The shape and dimensions of the deformed area have not changed significantly up to a relatively big depth.

In step 3 the cracks have the shape of a cross, with almost perpendicular arms. Different shapes of the cracks in step 3 (Fig. 4) were also noticed. The deformed area and the corresponding depth profile of the crack are shown in Fig. 5. Each dot represents one measured value.

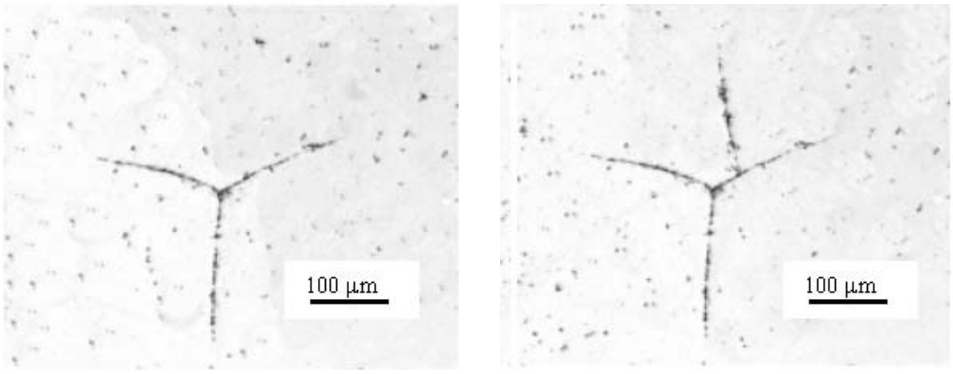

Fig. 4. Various shapes of cracks in step 3 (see Fig. 3).

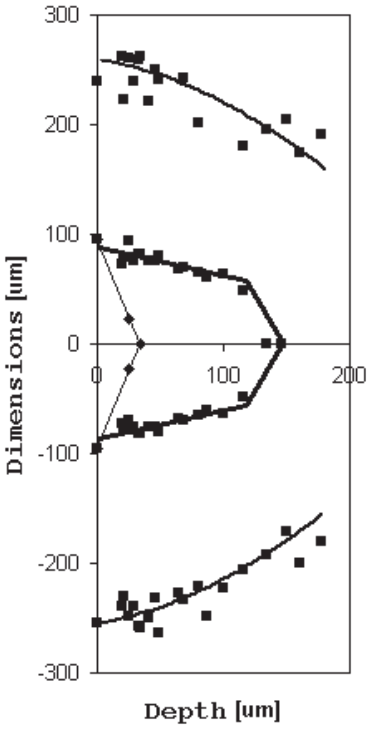

Fig. 5. Deformed area and corresponding depth profile of the crack.

The fracture surface below the indent can be seen in Fig. 6. The shape of the "remainder" of the indent is indicated by arrow 1. The deformed area (arrow 2) is placed asymmetrically under the indent. This asymmetry with respect to the position of the indent can be seen also in the depth profile of the cracks (arrow 3). The shape of the deformed area is mostly block-like, with a sharp pyramidal tip. Figures 7a and 7b show two extreme shapes – purely pyramidal and almost spherical, respectively. In Fig. 7b a part of the deformed area seems to be cracked off, what makes the definition of the shape more complicated. The deformed area is a region with large amount of defects, with some cracks inside (indicated by arrows 1 in Fig. 7).

The shape of the deformed area has been considered circular [10], with a lateral crack underneath, as seen in Fig. 8. The formula to determine the depth of the deformed area (in mm) [11] is as

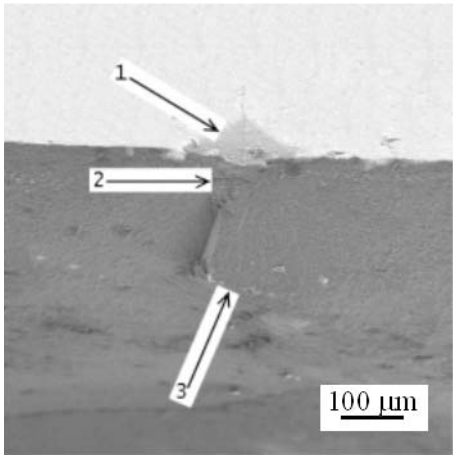

Fig. 6. Fracture area of the specimen: 1 – indent, 2 – deformed area, 3 – depth profile of the crack.

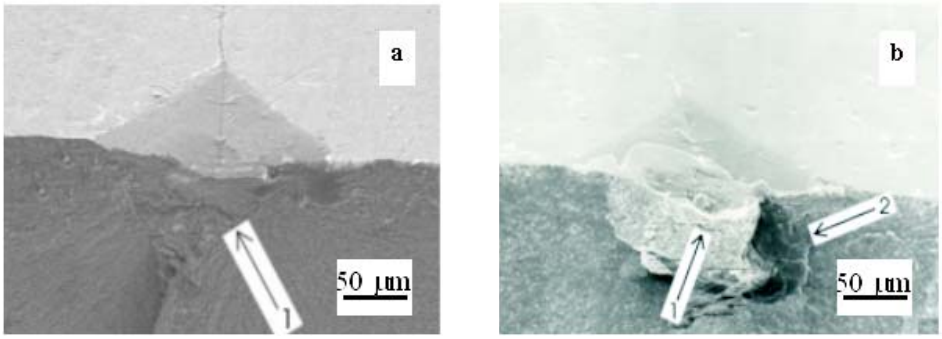

Fig. 7. Various shapes of the deformed areas. Arrows 1 indicate cracks inside the deformed area. Arrow 2 indicates the assumed remainder of a lateral crack.

follows:

$$h \approx \left(\frac{p}{H}\right)^{\frac{1}{2}} \cdot \left(\frac{E}{H}\right)^{\frac{2}{5}}, \tag{2}$$

where p is indentation loading force [N], H is Vickers hardness [MPa], E is Young's modulus of elasticity [MPa].

None of the above assumptions has been proved by our experiments. The shape of the deformed area is angular rather than circular, with no lateral cracks identified underneath during the ablation. No lateral cracks were identified in the fracture areas, except for the one shown in Fig. 7b, arrow 2, which could be considered as a remainder of a lateral crack. The depth of the deformed area calculated from

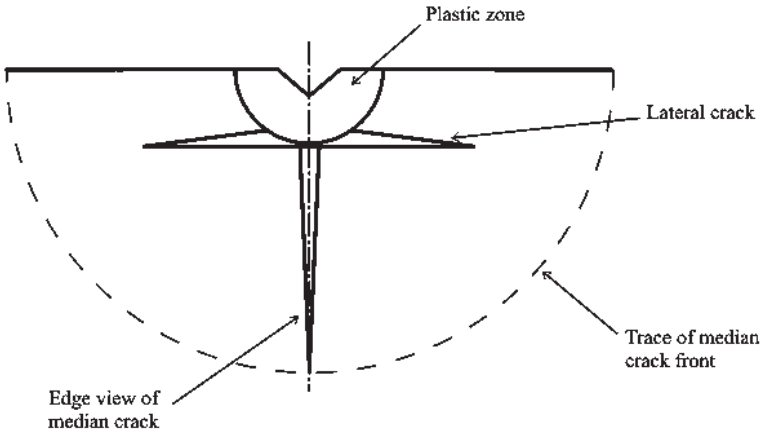

Fig. 8. Original assumption of the shape of the fracture area.

formula (2) (with $E = 310$ GPa) is more than 400 μm, the depth obtained from the experiment and from the observation of the fracture areas ranges only from 120 to 140 μm.

Next step in the study of the deformed area was to compare its volume with the volume of the indent. The considered shape of the deformed area consists of two parts: a truncated pyramid with both bases of similar surface area and a pyramidal tip. The model is shown in Fig. 9.

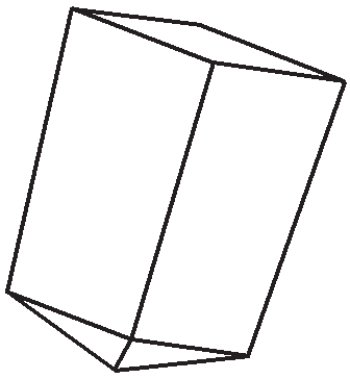

Fig. 9. Considered shape of the deformed area (3D model sketch).

Using basic geometrical formulae we calculated the volume of these bodies. These volumes have been then compared with the volumes of the indents. The volume of the indent represents on average 8 % of the volume of the deformed area, taking into account the mean values from two specimens (Fig. 10). A hypothesis has been taken into account, that the deformed area could have been created by filling cavities and defective regions inside the material. The defective regions consist of residual porosity after hot pressing and most probably also of the cracked off volumes of binding phase YAG. This binding phase is very brittle and the mechanism of its cracking off has been confirmed in

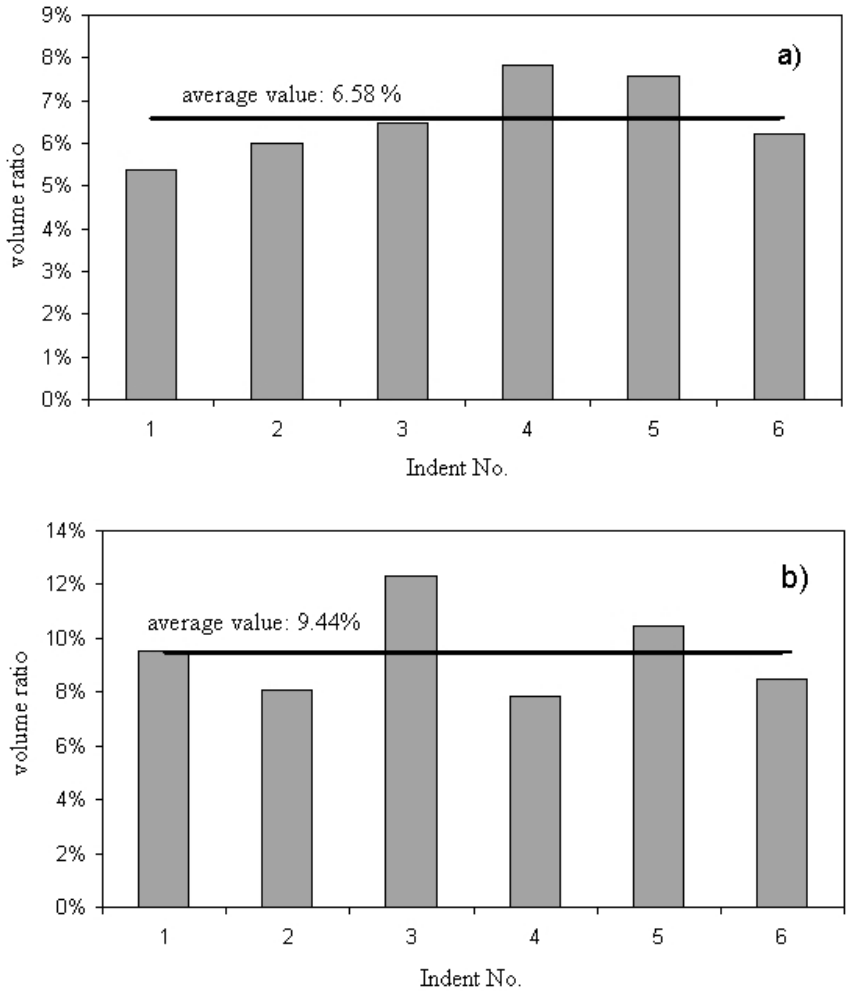

Fig. 10. Volume ratio of the volume of the indent and the volume of the deformed area. a) Specimen 1, b) Specimen 2.

work [12], which was dealing with abrasion resistance of our experimental material. The area of the defective regions was measured from pictures and (expressed in %) subsequently considered as their volume.

Two specimens have been used in this experiment and both of them showed high deviations (up to 20 %) from an average value of 5.3 %. However, in Fig. 3 it can be seen, that the volume of defective regions is much higher under the surface (after sectioning) than on the surface. The content in these layers is approximately

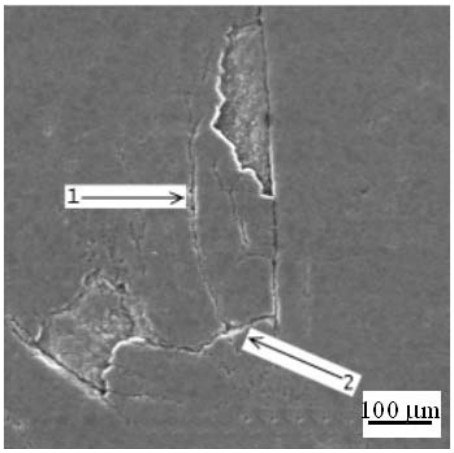

Fig. 11. A minor crack (1), a crack on the interface of the deformed and undeformed area (2).

9 %, which corresponds with the volume ratio in Fig. 10. Comparing the volume ratio of the deformed areas and indents with the volume content of defective regions makes the above hypothesis possible. However, a question where could the binding phase YAG crack off during the indentation still remains open.

At the determination of the depth profile of the cracks (Fig. 3), there were also other cracks observed, which were shorter but more numerous and will be referred to as minor cracks. A minor crack is shown in Fig. 11, which (as all the others) originates from the interface between deformed and non-deformed area. The depth of these cracks corresponds with the depth of the indent in some cases, but mostly it is bigger – however, their depth is never bigger than the depth of the deformed area.

4. Conclusions

The achieved results can be summarized in following points:

– The shape of the deformed area under the indent is mostly angular, of a block-like shape with a pyramidal tip, with shapes varying from purely pyramidal to almost spherical. Original assumption of the shape of the deformed area has not been proved.

– The depth of the deformed area ranges from 120 to 140 μm. The depth calculated from an original formula (400 μm) has not been proved.

– The ratio of volume of the indent and the volume of deformed area is in good agreement with the volume of the defective regions under the surface.

– Minor cracks have been registered on the interface of deformed and non-deformed area. These cracks are shorter than the major ones, but more numerous and their depth never exceeded the depth of the deformed area.

REFERENCES

[1] PÁNEK, Z.—FIGUSCH, V.—HAVIAR, M.—LIČKO, T.—ŠAJGALÍK, P.— DUSZA, J.: Konštrukčná keramika. Bratislava, R&D 1992.
[2] HVIZDOŠ, P.—KAŠIAROVÁ, M.—DUSZA, J.—HNATKO, M.—ŠAJGALÍK, P.: Kovove Mater., *42*, 2004, p. 51.
[3] KOVALČÍK, J.—HVIZDOŠ, P.—DUSZA, J.—ŠAJGALÍK, P.—HNATKO, M.—REECE, M.: Kovove Mater., *41*, 2003, p. 377.
[4] GONDÁR, E.—PULC, V.—KRIŽANSKÁ, M.: In: Proceedings Technologia 95. SjF STU Bratislava, p. 34.
[5] GONDÁR, E.: The testing method of resistance of silicon nitride based technical ceramics to thermal loading. [Conferment project]. Bratislava, SjF STU 1998.
[6] DUSZA, J.: Scripta Met. et Mat., *26*, 1992, p. 337.
[7] LUBE, T.: J. Eur. Ceram. Soc., *21*, 2001, p. 211.
[8] PULC, V.—GONDÁR, E.—ŠVEC, P.: In: Proceedings CO-MAT-TECH '93. MtF STU Trnava, p. 96.
[9] PULC, V.—GONDÁR, E.—ŠVEC, P.: In: International Conference 1992, SjF TU Košice, p. 97.
[10] HORVÁTHOVÁ, J.—OLEJNÍČKOVÁ, L.—JONSTA, Z.—MAZANEC, K.: In: Proceedings Fractography 2003. Institute of Material Research SAV Košice, p. 94.
[11] EVANS, A. G.—WILSHAW, T. R.: Acta Metall., *24*, 1976, p. 939.
[12] BRUSILOVÁ, A.: The study of abrasion resistance of silicon nitride based technical ceramics. [Thesis project]. Bratislava, SjF STU 2003.